Journal of Nanoscience and Nanotechnology
Vol. 9, 6434–6438, 2009

X-ray Magnetic Circular Dichroism and Small Angle Neutron Scattering Studies of Thiol Capped Gold Nanoparticles

J. de la Venta[1,2,*], V. Bouzas[1], A. Pucci[3], M. A. Laguna-Marco[4], D. Haskel[4], S. G. E. te Velthuis[6], A. Hoffmann[5,6], J. Lal[7], M. Bleuel[7], G. Ruggeri[3], C. de Julián Fernández[8], and M. A. García[1]

[1] *Dpto. Física de Materiales, Universidad Complutense de Madrid, 28040 Madrid, Spain*
[2] *Instituto de Magnetismo Aplicado UCM, 28230 Las Rozas, Madrid, Spain*
[3] *Department of Chemistry and Industrial Chemistry, University of Pisa, Via Risorgimento, 35 56126 Pisa, Italy*
[4] *Advanced Photon Source, Argonne National Laboratory, Argonne, Illinois 60439, USA*
[5] *Materials Science Division, Argonne National Laboratory, Argonne, Illinois 60439, USA*
[6] *Center for Nanoscale Materials, Argonne National Laboratory, Argonne, Illinois 60439, USA*
[7] *Intense Pulsed Neutron Source, Argonne National Laboratory, Argonne, Illinois 60439, USA*
[8] *Laboratorio di Magnetismo Molecolare, INSTM, UdR Firenze, via della Lastruccia 3, 50019 Sesto Fiorentino, Italy*

X-ray magnetic circular dichroism (XMCD) and Small Angle Neutron Scattering (SANS) measurements were performed on thiol capped Au nanoparticles (NPs) embedded into polyethylene. An XMCD signal of $0.8 \cdot 10^{-4}$ was found at the Au L_3 edge of thiol capped Au NPs embedded in a polyethylene matrix for which Superconducting Quantum Interference Device (SQUID) magnetometry yielded a saturation magnetization, M_S, of 0.06 emu/g_{Au}. SANS measurements showed that the 3.2 nm average-diameter nanoparticles are 28% polydispersed, but no detectable SANS magnetic signal was found with the resolution and sensitivity accessible with the neutron experiment. A comparison with previous experiments carried out on Au NPs and multilayers, yield to different values between XMCD signals and magnetization measured by SQUID magnetometer. We discuss the origin of those differences.

Keywords: Gold Nanoparticles, X-ray Magnetic Circular Dichroism (XMCD), Small Angle Neutron Scattering (SANS).

1. INTRODUCTION

One of the basic tenets of nanoscience is that the physical properties of the materials are modified when their size is reduced to the nanoscale. These changes arise mainly from the fact that the nanoscale materials have a relatively large fraction of surface atoms (this fraction is negligible for bulk materials), and from geometric confinement effects. The later occur when the characteristic length scale of a given phenomenon transgresses the particle size, and consequently the response of the system becomes strongly dependent on its size (that is, on the boundary conditions).

Surface atoms do not only reside in a different crystalline environment compared to the bulk atoms but they can also readily be modified through bonds with other species, providing a method to tune their physical properties. An example for nanoscale surface-induced magnetism is the appearance of ferromagnetic-like behavior in Au NPs capped with thiols[1–6] or other surfactants.[7,8] While the effect has been reproduced in samples prepared in different ways,[1,2] the experimental results reported independently by several groups are varying in detail,[1,6,9] ranging from the temperature independent ferromagnetic-like behavior observed in previous experiments to the superparamagnetic behavior in Au NPs reported by Dutta et al.[6] Even giant magnetic moments have been found in Au thin films with self-assembled layer of thiols adsorbed at the surface.[9] The origin of this magnetism remains still unresolved.[10,11] The bond between the sulphur atoms at the end of the thiol chain and the Au atoms at the NPs surface induces a charge transfer (as measured by XANES) from the Au to the S atom,[12] creating an open 5d electronic configuration in the surface of Au NPs[13] required for magnetism.

*Author to whom correspondence should be addressed.

 1533-4880/2009/9/6434/005 doi:10.1166/jnn.2009.1877

XMCD can be a key tool to elucidate the origin of this magnetism due to its unique features including element sensitivity and the possibility to separate orbital and spin contributions to the magnetization. SANS is appropriate to investigating structure and magnetic properties at the nanoscale due to the well-matched wavelength of neutrons from 0.05 nm to 20 nm. SANS can be used to obtain information about the size and dispersion of the NPs, as well as to probe for magnetic ordering at various length scales. The aim of this work is to characterize the structural and magnetic properties of Au NPs using SANS and XMCD measurements with the aim of understanding the origin of the unusual magnetism when the NPs are capped with thiol capping agents.

2. EXPERIMENTAL DETAILS

Dodecanethiol-capped Au NPs were prepared as described in the literature following a bottom-up approach.[2, 14] Briefly, polymeric Au nanocomposites (Au NPs-PE film) were prepared by casting a solution of 4 wt% of Au NPs and ultra high molecular weight polyethylene (UHMWPE, Stamylan UH210, supplied by DSM, The Netherlands) in *p*-xylene at 125 °C, and recovering the film after solvent evaporation at room temperature.

Bright-field transmission electron microscopy (TEM) pictures were obtained of Au NPs embedded into PE matrix (sixty-nanometer thin cuts were performed in a Leica Reichert Ultracut ultramicrotome, using a Diatome diamond knife and collected over 300 mesh copper grids).[14] Magnetic characterization of the samples was carried out with a SQUID magnetometer.

The X-ray measurements were carried out at beamline 4-ID-D of the Advanced Photon Source at Argonne National Laboratory.[15] A toroidal Pd focusing mirror was used to focus the central 1×1 mm^2 portion of the undulator beam to a 120×180 μm^2 spot size. Circularly polarized X-rays were generated by a 540 μm-thick diamond phase-retarding crystal operated in Bragg-transmission geometry.[16, 17] The XMCD was measured by modulating the X-ray helicity at 12.7 Hz and detecting the related modulation in the absorption coefficient with a lock-in amplifier. Measurements were performed with field $H =$ 4 T and $H = -4$ T.

SANS experiments in thiol-capped Au NPs in powder form were performed on the SASI instrument of the Intense Pulsed Neutron Source, Argonne National Laboratory on a sample with a dilute concentration of $c =$ 0.011 g/ml of Au NPs in deuterated Toluene. Measurements were performed with $H = 0$ T and with $H = 0.85$ T applied vertically.

3. RESULTS

Bright-field transmission electron microscopy (TEM) shows mostly spherical shaped particles with a mean size of about 3–4 nm (Fig. 1). Particularly, Au NPs are well dispersed inside the polymer matrix thanks to the dodecanethiol protecting layer that prevented particle aggregation during film preparation at high temperature.

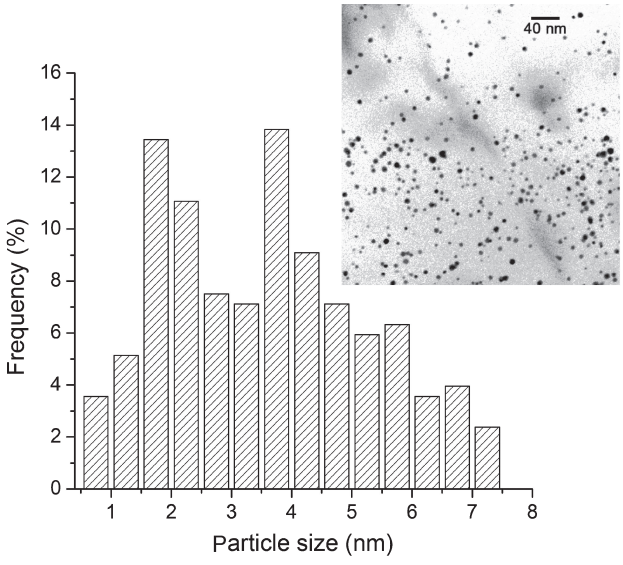

Fig. 1. Particle size distribution of 4 wt% Au NPs-PE film. Inset shows the bright-field transmission electron micrograph.

Magnetic characterization of the sample is presented in Figure 2. The diamagnetic contribution of the sample holder was previously measured and removed from the total magnetization. The polyethylene matrix was also measured and presents a pure diamagnetic behavior. Figure 2 shows the hysteresis loops of the sample at 300 K. In order to obtain only the contribution of the gold NPs, the diamagnetic signal of the polyethylene was subtracted.

Although the NPs are only 4 wt% of the total sample their magnetic moments are large enough to overcome the diamagnetism from the polyethylene matrix and the inner core of the Au NPs for fields below 4000 Oe (Fig. 2).

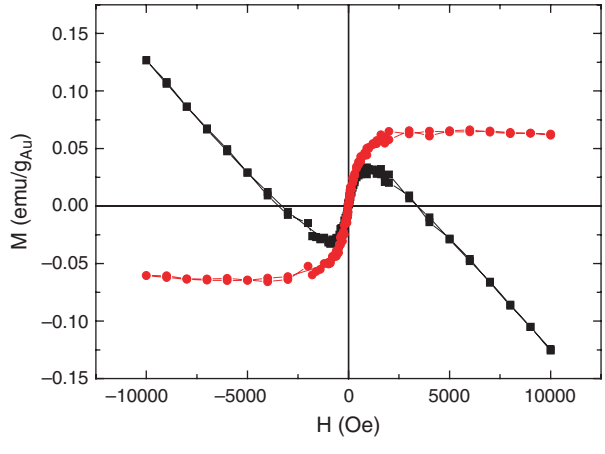

Fig. 2. (black squares) Magnetization curves of the sample at 300 K and (red dots) the contribution of Au NPs-PE film after subtracting the diamagnetic matrix component.

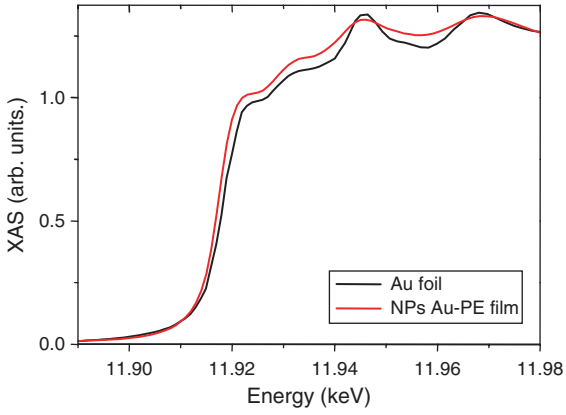

Fig. 3. XAS spectra at Au L_3 edge for the Au NPs-PE film and Au foil.

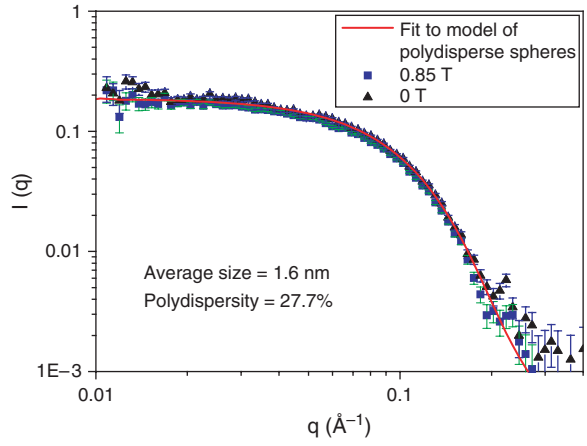

Fig. 5. SANS for the Au NPs, showing the isotropic average of the scattered intensity I as a function of momentum transfer q.

Coercive field at 300 K is about 20 Oe, confirming the presence of hysteresis at room temperature. The curves are identical at 5 K and 300 K[2] and the magnetization is constant over this interval of temperature. The saturation magnetization M_S is 0.06 emu/g_{Au} which correspond to $2.11 \cdot 10^{-3}$ μ_B/Au atom.

XAS spectra at the L_3 edge of Au (electric dipole transition 2p→5d) from the sample and a reference Au metal foil are presented in Figure 3. The differences confirm the charge transfer from Au to S when thiols are attached to the nanoparticle in agreement with previous results.[1, 12]

Figure 4 presents XMCD results at the L_3 edge of Au. The data is an average over 66 scans (33 scans with field $H = +4$ T and 33 scans with $H = -4$ T, the field reversed every 3 scans), at two different temperatures, 4.3 K and 300 K. Since magnetization-reversal is equivalent to helicity switching, measurements with opposite field direction can be combined to remove any spurious signal of non-magnetic origin. A clear XMCD signal was found in the sample for both temperatures. The main peak is located at $E = 11.918$ keV with amplitudes of $(0.8 \pm 0.1) \cdot 10^{-4}$ at 300 K and $(1 \pm 0.1) \cdot 10^{-4}$ at 4.3 K. An additional smaller peak was also found at $E = 11.931$ keV, with amplitudes of $(0.5 \pm 0.1) \cdot 10^{-4}$ at 4.3 K and 300 K.

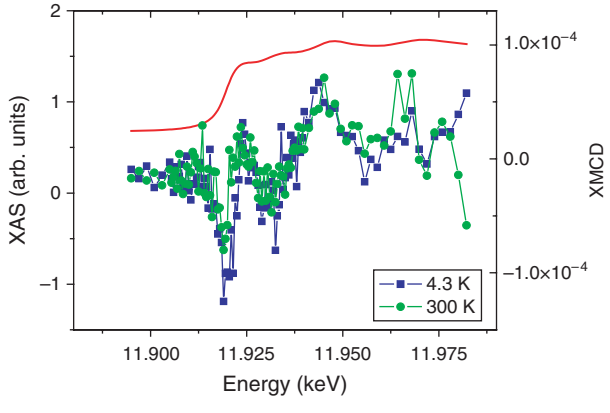

Fig. 4. XAS (shifted) and XMCD spectra at the Au L_3 edge for Au NPs-PE film measured in transmission mode.

The SANS data at both applied magnetic fields was isotropically distributed in all scattering directions and coincided, indicating that there was no detectable magnetic contrast at the resolution and sensitivity accessible with the experiment, due to the small size of the particles and the small values of the magnetization. Although the particles are not embedded in the polymer, the size and magnetic response measured by SQUID is the same than when they are dispersed in PE-film. From fits to the data (Fig. 5) with a model of polydisperse spheres it was determined that the particles have an average radius of 1.6 nm, i.e., 3.2 nm of diameter, with a 27.7% polydispersity.

4. DISCUSSION

It has been observed that NPs in powder form after some months have partially sintered.[18] This fact has a direct effect on the magnetic behavior, since the magnetic signal decreases after this period, typically about 50% after three months. On the other hand, the particles embedded in the PE film are very stable and do not show aggregation effects and the magnetic response is stable with time. Besides they have the advantage of simple handling as well as easy sample preparation.

Comparing the observed XMCD signal with previous results, Yamamoto et al. found magnetization in the 5d orbital of Au NPs protected with polyallylamine hydrochloride (PAAHC),[7] which exhibited paramagnetic behavior. They found two peaks at the Au L_3 edge at the same positions as those reported here. The magnetization at 2.6 K under an applied field of 10 T was 0.035 emu/g_{Au} (corresponding to $1.0 \cdot 10^{-3}$ μ_B/Au atom) and for this field and temperature they found an XMCD signal at the Au L_3 edge of $3.0 \cdot 10^{-4}$. This experiment performed at the BL39XU beamline in SPring-8 gave a ratio of $1.16 \cdot 10^2$ emu $\cdot$ g_{Au}/XMCD.

This ratio is quite similar to that found by Wilhelm et al. on Au/Co multilayers[19] in experiments carried out at beamline ID12 at the ESRF, where an XMCD signal of 0.007 was found at the L_3 edge. The analysis provides values for the magnetic moment in the Au of about 0.03 μ_B/Au atom (0.8 emu/g_{Au}), this yields a ratio between the magnetization and XMCD signal of $1.33 \cdot 10^2$ emu $\cdot$ g_{Au}/XMCD. The shape of the XMCD peak is very similar for both measurements although they are shifted by 13 eV (the maximum correspond to 11930 eV for ESRF and 11917 for SPring-8) which is likely due to different energy calibrations.

For thiol capped Au NPs-PE film, the position of the XMCD signals, the shape and the amplitude agree with the measurements reported by Yamamoto et al. The amplitude of the signal is similar at 300 K and 5 K. In our samples the M_S value (0.06 emu/g_{Au}) corresponds to $2.11 \cdot 10^{-3}$ μ_B/atom Au. The XMCD signal at 5 K is $1 \cdot 10^{-4}$. With these values we obtain an emu $\cdot$ g_{Au}/XMCD ratio of $6 \cdot 10^2$, which is five times larger but within the same order of magnitude as the results from the previous work.

Next we discuss the origin of the magnetic moments in the three sets of samples described above. In Co/Au multilayer reported by Wilhelm et al., the XMCD signal is related to the presence of neighboring magnetic atoms, i.e., the Au magnetic polarization is due to proximity effects mediated by 5d–3d hybridization. Magnetic polarization in Yamamoto paramagnetic NPs[7] appears when the NPs are capped with weakly interacting molecules. Thus the effect is related with a reduction in the size. The observed magnetism in thiol capped Au NPs is different to that found in the PAAHC Au NPs. They found a mixture of superparamagnetic and paramagnetic contributions, while thiol capped Au NPs present a temperature independent ferromagnetic-like behavior. For these latter NPs the magnetic ordering seems related to the strong bonding between Au NP and thiol surfactants.

Although the interaction of the Au NPs with the surrounding media is different (weakly interacting molecule in PAAHC Au NPs and strongly interacting capping agent for thiol capped Au NPs), the ratios between SQUID and XMCD measurements are of the same order of magnitude. This suggests that in both samples the magnetism is localized in the 5d orbital.

In a recent experiment Garitaonandia et al.[20] also found a net magnetization in thiol capped Au NPs with M_S of 5 emu/g_{Au} (that corresponds to 0.18 μ_B/atom). XMCD measurements performed at BL39XU beamline in SPring-8 showed a signal of $7 \cdot 10^{-5}$, resulting in $7.15 \cdot 10^4$ emu $\cdot$ g_{Au}/XMCD, about two orders of magnitude larger than the three experiments discussed earlier.

Theoretical calculations obtained a magnetic moment of 0.0025 μ_B per S–Au bond for a system consisting on a small cluster of 13 gold atoms and one chemisorbed molecule. C_6H_6–S–Au_{13}.[21] This result in very good agreement with the value of 0.0021 μ_B/atom obtained for our samples but is at odds with the large value reported by Garitaonandia et al.

Hence, the results in our samples can be explained as due to the polarization of 5d orbitals in gold atoms. On the other hand, the large SQUID values and small XMCD signals found by Garitaonandia et al. suggests that the SQUID data contains magnetic contributions from sources other than Au 5d magnetism.

The idea of magnetic polarization beyond the 5d orbital in thiol capped Au surfaces has been previously suggested. Vager and Naaman[10] proposed orbital magnetism from electrons in the self-assembled layer of thiols. Hernando et al.[11,22] proposed that conduction electrons of Au can occupy orbits around a small blocked spin localized in the bond Au–S due to the charge transfer experimentally observed in these bonds. These orbital magnetic moments atoms could reach giant values (in the order of tens of μ_B per surface atoms). Although our results can be explained by purely 5d magnetism, we can not discard the existence of other contributions for other related nanostructures.

5. CONCLUSIONS

We carried out XMCD measurements at the Au L_3 edge of thiol capped Au NPs embedded in a polyethylene matrix. A XMCD signal was found, with amplitudes of $1 \cdot 10^{-4}$ for samples with M_S of 0.06 emu/g_{Au} as measured with a SQUID. Therefore, the results demonstrate that there is Au magnetization in thiol capped Au NPs, localized in the 5d orbital of Au atoms. Comparison with previous results indicates that the $2.11 \cdot 10^{-3}$ μ_B/Au atom magnetism is localized on the 5d orbital of Au atoms. Nevertheless the existence of other magnetic contributions beyond this orbital can not be completely ruled out.

The fact that no magnetization was detected in the SANS experiment, does not discard the presence of magnetic order. A higher resolution as well as larger magnetic signal of the particles may enable future more sensitive neutron measurements.

Acknowledgments: A. Hernando, Pietro Gambardella, Stefano Rusponi are acknowledged for fruitful discussion and valuable comments. E. Fernández Pinel is acknowledged for technical suggestions and advice. This work has been partially supported by the EU (project "BONSAI" LSHB-CT-2006-037639). M. A. Laguna-Marco acknowledges MEC for postdoctoral fellowship. Work at Argonne was supported by the U.S. Department of Energy, Office of Basic Energy Sciences, under Contract No. DE-AC02-06CH11357.

References and Notes

1. P. Crespo, R. Litrán, T. C. Rojas, M. Multigner, J. M. de la Fuente, J. C. Sánchez-López, M. A. García, A. Hernando, S. Penadés, and A. Fernández, *Phys. Rev. Lett.* 93, 087204 **(2004)**.
2. J. de la Venta, A. Pucci, E. Fernández-Pinel, M. A. García, C. De Julián, P. Crespo, G. Ruggeri, and A. Hernando, *Adv. Mat.* 19, 875 **(2007)**.
3. E. Guerrero, T. C. Rojas, M. Multigner, P. Crespo, M. A. Muñoz-Márquez, M. A. García, and A. Hernando, *Acta Mat.* 55, 1723 **(2007)**.
4. P. Crespo, M. A. García, E. Fernández Pinel, M. Multigner, D. Alcántara, J. M. de la Fuente, S. Penadés, and A. Hernando, *Phys. Rev. Lett.* 97, 177203 **(2006)**.
5. J. De La Venta, E. Fernandez Pinel, M. A. Garcia, P. Crespo, A. Hernando, O. Rodriguez De La Fuente, C. De Julián Fernández, A. Fernández, and S. Penadés, *Mod. Phys. Lett. B* 21, 303 **(2007)**.
6. P. Dutta, S. Pal, M. S. Seehra, M. Anand, and C. B. Roberts, *Appl. Phys. Lett.* 90, 213102 **(2007)**.
7. Y. Yamamoto, T. Miura, M. Suzuki, N. Kawamura, H. Miyagawa, T. Nakamura, K. Kobayashi, T. Teranishi, and H. Hori, *Phys. Rev. Lett.* 93, 116801 **(2004)**.
8. P. de la Presa, M. Multigner, J. de la Venta, M. A. García, and M. L. Ruiz Gonzalez, *J. Appl. Phys.* 100, 123915 **(2006)**.
9. I. Carmeli, G. Leitus, R. Naaman, S. Reich, and Z. Vager, *J. Chem. Phys.* 18, 10372 **(2003)**.
10. Z. Vager and R. Naaman, *Phys. Rev. Lett.* 92, 087205 **(2004)**.
11. A. Hernando, P. Crespo, and M. A. Garcia, *Phys. Rev. Lett.* 96, 057206 **(2006)**.
12. P. Zhang and T. K. Sham, *Phys. Rev. Lett.* 90, 245502 **(2003)**.
13. M. A. Garcia, J. de la Venta, P. Crespo, J. LLopis, S. Penadés, A. Fernández, and A. Hernando, *Phys. Rev. B* 72, 241403(R) **(2005)**.
14. A. Pucci, N. Tirelli, E. A. Willneff, S. L. M. Schroeder, F. Galembeck, and G. Ruggeri, *J. Mater. Chem.* 14, 3495 **(2004)**.
15. J. W. Freeland, J. C. Lang, G. Srajer, R. Winarski, D. Shu, and D. M. Mills, *Rev. Sci. Instrum.* 73, 1408 **(2002)**.
16. K. Hirano, K. Izumi, T. Ishikawa, S. Annaka, and S. Kikuta, *J. Appl. Phys.* 30, L407 **(1991)**.
17. J. C. Lang and G. Srajer, *Rev. Sci. Instrum.* 66, 1540 **(1995)**.
18. C. J. Kiely, J. Fink, M. Brust, D. Bethell, and D. J. Schiffrin, *Nature* 396, 444 **(1998)**.
19. F. Wilhelm, M. Angelakeris, N. Jaouen, P. Poulopoulos, E. Th. Papaioannou, Ch. Mueller, P. Fumagalli, A. Rogalev, and N. K. Flevaris, *Phys. Rev. B* 69, 220404 **(2004)**.
20. J. S. Garitaonandia, M. Insausti, E. Goikolea, M. Suzuki, J. D. Cashion, N. Kawamura, H. Ohsawa, I. Gil de Muro, K. Suzuki, F. Plazaola, and T. Rojo, *Nano Lett.* 8, 661 **(2008)**.
21. C. Gonzalez, Y. S. Manso, M. Marquez, and V. Mujica, *J. Phys. Chem. B* 110, 687 **(2006)**.
22. A. Hernando, P. Crespo, M. A. García, E. Fernández Pinel, J. de la Venta, A. Fernández, and S. Penadés, *Phys. Rev. B* 74, 052403 **(2006)**.

Received: 5 February 2009. Accepted: 7 April 2009.